Enhanced SRSF5 Protein Expression Reinforces Lamin A mRNA Production in HeLa Cells and Fibroblasts of Progeria Patients

Valentin Vautrot, Christelle Aigueperse, Florence Oillo-Blanloeil, Sebastien Hupont, James Stevenin, Christiane Branlant, Isabelle Behm-Ansmant

Enhanced SRSF5 protein expression reinforces lamin A mRNA production in HeLa cells and fibroblasts of progeria patients

Valentin Vautrot[1+], Christelle Aigueperse[1+], Florence Oillo-Blanloeil[1], Sébastien Hupont[3], James Stevenin[2], Christiane Branlant[1*] and Isabelle Behm-Ansmant[1*]

[1] IMoPA (Ingénierie Moléculaire et Physiopathologie Articulaire), UMR 7365 CNRS-UL, Biopôle de l'Université de Lorraine, 9 Avenue de la forêt de Haye, 54505 Vandoeuvre-lès-Nancy

[2]IGBMC Department of Functional Genomics and Cancer, CNRS UMR 7104, INSERM U 964, University of Strasbourg, 1 Rue Laurent Fries, 67404 Illkirch Cedex, France

[2]FR3209 CNRS, Biopôle de l'Université de Lorraine, 9 Avenue de la forêt de Haye, 54505 Vandoeuvre-lès-Nancy

+ These two authors contributed equally to this work

Running title: SRSF5 regulates LMNA exon 11 splicing

* To whom correspondence should be addressed:

isabelle.behm@univ-lorraine.fr

christiane.branlant@univ-lorraine.fr

Grant sponsor: Agence Nationale de la Recherche (ANR-05-BLAN-0261-01); European Alternative Splicing Network of Excellence (EURASNET, FP6 life sciences, genomics and biotechnology for health); Région Lorraine (PRST IMTS)

ABSTRACT (200 words)

The Hutchinson Gilford Progeria Syndrome (HGPS), is a rare genetic disease leading to accelerated aging. Three mutations of the *LMNA* gene leading to HGPS were identified. The more frequent ones, c.1824C>T and c.1822G>A, enhance the use of the intron 11 progerin 5ôsplice site (5ôSS) instead of the LMNA 5ôSS, leading to the production of the truncated dominant negative progerin. The less frequent c.1868C>G mutation creates a novel 5ôSS (LAΔ35 5ôSS), inducing the production of another truncated LMNA protein (LAΔ35). Our data show that the progerin 5ôSS is used at low yield in the absence of HGPS mutation, while utilization of the LAΔ35 5ôSS is dependent upon the presence of the c.1868C>G mutation. In the perspective to correct HSPG splicing defects, we investigated whether SR proteins can modify the relative yields of utilization of intron 11 5ôSSs. By *in cellulo* and *in vitro* assays, we identified SRSF5 as a direct key regulator increasing the utilization of the LMNA 5ôSS in the presence of the HGPS mutations. Enhanced SRSF5 expression in dermal fibroblasts of HGPS patients as well as PDGF-BB stimulation of these cells decreased the utilization of the progerin 5ôSS, and improves nuclear morphology, opening new therapeutic perspectives for premature aging.

Keywords: alternative splicing; Hutchinson Gilford Progeria Syndrome; SRSF5; SRSF1; PDGF-BB, *LMNA*

INTRODUCTION

The Hutchinson Gilford Progeria Syndrome (HGPS), also called progeria, is a rare genetic disease leading to premature aging. Progeria is caused by mutations in the *LMNA* gene (OMIM accession number 150330), coding lamin A, a protein of the nuclear envelope substructure called lamina. The nuclear lamina is a major element in coordinating the mechanical properties of the nucleus, the regulation of gene expression and genome maintenance [Goldberg et al., 1999]. The most frequent mutation responsible for progeria is the silent c.1824C>T (p.G608) mutation, leading to the excision of intron 11 by utilization of an alternative 5ô-splice site, the progerin 5ô-splice site (hereafter designated as progerin 5ôSS) [De Sandre-Giovannoli et al., 2003; Eriksson et al., 2003]. This site is used at very low level in normal human cells [Scaffidi and Misteli, 2006]. As it is located 150 nts upstream from the canonical site (LMNA 5ôSS), a truncated version of the lamin A protein is produced (progerin or LAΔ50). Progerin retains the C-terminal CAAX box of Lamin A, which undergoes methyl esterification and farnesylation, but lacks amino acids essential for one of the specific cleavage steps of the lamin A maturation pathway [De Sandre-Giovannoli, et al., 2003; Eriksson, et al., 2003; Dechat et al., 2007]. Consequently, progerin is permanently farnesylated and carboxymethylated, which leads to its abnormal anchoring to the nuclear membrane throughout the cell cycle [Glynn and Glover, 2005; Dechat, et al., 2007; Cao et al., 2007]. Nuclear accumulation of progerin interferes with nuclear lamina integrity, causing misshapen nuclei. It also adversely affects other important cellular processes, such as interphase chromatin, mitosis and cell proliferation [Scaffidi and Misteli, 2008; Shumaker et al., 2006; Cao, et al., 2007]. Among the few other mutations within the LMNA gene which are leading to HGPS or HGPS-like syndromes [Eriksson, et al., 2003; Fukuchi et al., 2004; Navarro et al., 2004; Moulson et al., 2007; Hisama et al., 2011; Barthelemy et al., 2015], the c.1822G>A (p.G608S) variation also activates the progerin 5ôSS, inducing progerin production. The c.1868C>G (p.T623S) mutation creates a novel 5ô-splice site located

105 nts upstream from the LMNA 5ôSS, designated as LAΔ35 5ôSS, which induces the production of the LAΔ35 isoform [Fukuchi, et al., 2004; Shalev et al., 2007] (Figure 1). Production of LAΔ35 was initially described in a patient presenting the full range of progeria symptoms when he died at the age of 45. However, the onset of the disease appeared late (age of 12) and it took a longer time to develop full-blown HGPS [Fukuchi, et al., 2004].

HGPS is thus characterized by a defect of LMNA pre-mRNA processing by the spliceosome, which is the nuclear machinery responsible for intron removal from pre-mRNAs [Will and Luhrmann, 2001]. The assembly and activity of the spliceosome rely heavily on a dynamic of interactions established between five UsnRNPs (U1, U2, U4/U6 and U5 sRNPs), numerous proteins and the pre-mRNA [Wahl et al., 2009]. Formation of a base-pair interaction between U1 snRNA and the pre-mRNA 5ôSS region plays a crucial role in the initiation of spliceosome assembly, and the pattern of hydrogen bonds that can be established between the pre-mRNA 5ôSS and U1 snRNA is one key determinant of the 5ôSS intrinsic strength. However, this intrinsic strength is most often modulated by surrounding or overlapping regulatory sequences that recruit splicing regulatory proteins [Black, 2003], in particular, the heterogeneous ribonucleoproteins (hnRNPs) and proteins of the serine-arginine (SR)-protein family. In addition to their role in the basic mechanism of splicing, SR proteins play a critical role in the regulation of alternative splicing [Tazi et al., 2010; Bourgeois et al., 2004]. Alternative splicing is just as important as most of the human pre-mRNAs can be spliced differentially depending on developmental and physiological contexts. In addition, several genetic diseases are due to defects in alternative splicing [Gamazon and Stranger, 2014]. SR proteins are composed of one or two RNA recognition motif(s) (RRM) and an arginine-serine rich (RS) domain, which are required for RNA-binding and protein-protein interaction, respectively. Phosphorylation of RS domains affects the RNA and protein binding properties of SR proteins, as well as their intracellular localization. Furthermore, an increasing number of studies report modulations of

alternative splicing by signaling-activated kinases such as Akt. They either directly phosphorylate SR proteins or activate SR dedicated kinases, such as the SR protein kinases (SRPKs) or the CDC2-like kinase family (CLKs) [Naro and Sette, 2013].

In agreement with our previous data on the LMNA and progerin 5'SSs [Lopez-Mejia et al., 2011], the comparative computer analysis of the LMNA and progerin 5'SS strengths in the presence and the absence of HGPS mutations that we performed with three different algorithms with proven performance [Sharma et al., 2014], predict i) a high efficiency of the LMNA 5' SS in both the WT and the mutated genetic contexts, ii) a medium efficiency of the progerin 5' SS, and iii) a very low efficiency of the LAΔ35 5'SS in the WT context explaining the absence of use of this latter site (Figure 1). The c.1824C>T and c.1822G>A mutations are both predicted to increase the strength of the progerin 5'SS. Nevertheless, its score remains lower than those of the lamin A 5'SS (Figure 1). The c.1868C>G mutation is also predicted to increase the strength of the LAΔ35 5'SS, but here again, the scores, especially the SS score, are quite lower than those of the lamin A 5' SS. Therefore, the preferential utilization of the progerin or LAΔ35 5'SS in the presence of each of the HGPS mutations cannot be solely explained by variations of the intrinsic strengths of the various 5'SSs. Parameters other than complementarity with U1 snRNA should be involved in the reinforced utilization of the progerin and LAΔ35 5'SSs in the HGPS mutated contexts. Accordingly, our previous study demonstrated the contribution of the RNA 2D structure and the activity of two SR proteins to the progerin 5'SS selection in the presence of the progeria c.1824C>T mutation [Lopez-Mejia, et al., 2011].

These observations are very interesting as modulation of SR protein expression has already been shown to be an efficient strategy to correct alternative splicing defects linked to genetic diseases [Faustino and Cooper, 2003; Wee et al., 2014]. Here, we investigated whether the overexpression of various SR proteins can reduce the production of progerin or LAΔ35 mRNA in the presence of the c. 1824C>T, c.1822G>A or c.1868C>G mutation. By *in vitro* and *in*

cellulo assays, we identified the SR protein SRSF5 as an activator of the authentic LMNA 5ôSS and showed that an increased expression of SRSF5 in fibroblasts of HGPS patient favors the utilization of the LMNA 5ôSS at the expense of the progerin 5ôSS. Moreover, by PDGF-BB stimulation of HGPS fibroblasts, leading to an increased level of SR protein phosphorylation, we could partially correct the LMNA intron 11 splicing defect, reduce progerin production and induce partial recovery in the nuclear morphology of HGPS fibroblasts. This observation opens new therapeutic perspectives in the view to limit premature aging due to progerin production.

MATERIALS AND METHODS

Plasmids constructs

Following citations of the genomic mutations in the text, the HGVS mutation nomenclature referring to the main geneôs transcript coding sequence (NM_170707.3 for the *LMNA* gene) is preferred. Nucleotide numbering uses +1 as the A of the ATG translation initiation codon in this reference sequence, with the initiation codon as codon 1. The previously described pCDNA3.1/V5-His-TOPO plasmids [Lopez-Mejia et al., 2011] containing the WT or c.1824C>T **b***Glo*-LMNA construct were used for splicing experiments. The pCDNA3.1/V5-His-TOPO plasmids containing the c.1822G>A and c.1868C>G **b***Glo*-LMNA reporter genes (denoted 1822G>A and 1868C>G **b***Glo*-LMNA plasmids) were produced by site-directed mutagenesis (oligonucleotide sequences are available on request). The pXJ41 plasmid used for SR protein overexpression was previously described [Ropers et al., 2004].

Cell lines, culture and transfection assays

HeLa S3 cells were grown in Dulbeccoôs modified eagle medium (Gibco, Life Technologies, Saint-Aubin, France) complemented with 10% fetal calf serum (FCS) and antibiotics. Dermal fibroblasts from a female HGPS patient carrying the c.1824C>T mutation (AG11513) and from a healthy female (AG08470) (Coriell Cell Repositories, Camden, NJ, USA) were grown in

MEM medium (Gibco, Life Technologies, Saint-Aubin, France) complemented with 15% heat-inactivated FCS. One day before transfection, HeLa S3 cells were plated in six-well plates at ~200, 000 cells per well. They were co-transfected with 1.5 µg of one of the ***6****Glo*-LMNA plasmids and 10 to 250 ng of recombinant pXJ41 plasmid expressing one SR protein or an empty pXJ41 plasmid as a control. Co-transfection were achieved using JetPEI (Polyplus, Ozyme, Montigny le Bretonneux, France) according to the manufacturerôs instructions. The Amaxa NHDF Nucleofector Kit (Lonza, Basel, Switzerland) was used for transient transfection of HGPS dermal fibroblasts. Three micrograms of either empty pXJ41 or pXJ41-SRSF5 plasmid were added to 600, 000 cells in suspension and electroporation was achieved using the U-23 program. Cells were then plated into 6-well plates (300, 000 cells per well) and collected 24 hours later. Transfection efficiency was estimated by fluorescence-activated cell-sorting analysis of a co-transfected GFP expression vector. For PDGF-BB (Sigma, Saint-Louis, MO, USA) stimulation of HGPS dermal fibroblast, the cells were serum-starved (0,5 % FCS) for 48 hours and then stimulated 24 hours or daily for 4 days with PDGF-BB in serum-starved medium.

***In vitro* and *ex vivo* splicing assays**

Recombinant SR proteins were produced and purified from baculovirus-infected Sf9 cells as previously reported [Cavaloc et al., 1999]. *In vitro* splicing reactions were performed as previously described [Lopez-Mejia, et al., 2011]. Spliced products were analyzed by 6% polyacrylamide gel electrophoresis, and radioactive bands were quantified using the ImageQuant software.

For *ex vivo* splicing assays, RNA were extracted from the transfected cells using Trizol reagent (Ambion, Life Technologies, Saint-Aubin, France), then treated with RQ1 DNase (Promega, Charbonnieres, France). RNAs (0.5 to 1.5 µg) were reverse transcribed using random hexamer oligonucleotides and MMLV retrotranscriptase (Promega, Charbonnieres, France) according to

the manufacturer's instructions. PCR were carried out with 25 µM dNTP mix and 25U DreamTaq DNA pol (Fisher scientific, Illkirch, France) (oligonucleotides sequences are available on request). Denaturation, annealing and extension steps were performed for 30 s at 94, 65 and 72°C, respectively, for 35 cycles. The splicing products were fractionated on 2% agarose gel and quantified in four independent experiments using the GeneSnap acquisition and GeneTools analysis softwares (Syngene, Cambridge, UK).

Western blot analyses

To check for recombinant protein expression, the proteins from transfected HeLa cells and dermal fibroblasts were extracted in cell lysis buffer Tris-HCl 50 mM pH 8.0, NaCl 150 mM, 1% Igepal, EDTA 1 mM containing the Halt protease and phosphatase inhibitor cocktail EDTA-free (Pierce, Thermo Fisher Scientific Inc., Rockford, IL, USA). The supernatant was used for Western blotting to analyse of the level of expression of recombinant protein. Proteins were fractionated on 10% SDS-PAGE gels and transferred to 0.45 µm nitrocellulose membrane (Biorad). The following antibodies were used: anti-SRSF1 (Santa Cruz Biotechnology, Inc. #sc-73026), anti-SR (1H4) (Santa Cruz Biotechnology, Inc. #sc-13509), anti-SRSF7 (Euromedex #9G8-1C6), anti-PhosphoAkt (Ser473) (Cell Signaling Technology #4060), anti-lamin A/C (Santa Cruz Biotechnology, Inc. #sc-20681), anti-GAPDH (Abcam, #ab9485) and anti-β-tubulin I (Sigma #T7816) antibodies. After subsequent washing, membranes were incubated with HRP labeled goat anti-rabbit (Pierce, Thermo Fisher Scientific Inc., Rockford, IL, USA) or sheep anti-mouse immunoglobulins (Chemicon International Inc., Billerica, MA, USA) and incubated for 5 min with the chemi-luminescent substrate (ECL Prime kit, GE Healthcare, Velizy Villacoublay, France). Images were captured by a Fusion-Solo gel documentation system (Vilber Lourmat, Torcy, France) using the Fusion software.

Immunofluorescence experiments and image analysis

Cells were fixed in 4% paraformaldehyde in PBS and permeabilized with 0.5% Triton X-100 in PBS. To label Lamin A/C, cells were incubated with the primary antibody solution (Santa Cruz Biotechnology, Inc. #sc-20681, 1:30) for 1 h and then with the secondary antibody solution (Alexa fluor 488 goat anti-mouse, Invitrogen, 1:100) for 30 min. Imaging was performed using a Nikon Optiphot-2 fluorescence microscope. Changes in nuclear dysmorphic features (blebbing, invagination, or creasing) upon cell treatment with 40 ng/ml PDGF during 4 days, were estimated by a double-blinded nuclear counting assay by two independent personnel performed on four independent data sets of 150 to 270 lamin A/C labelled cells. For automated image analysis a custom-written Image J (National Institutes of Health, Bethesda, MD) script was used to extract nuclei boundaries and measure nuclei shape descriptors (solidity and aspect ratio). Full details on the automated image treatment procedure are provided in the Supplementary Methods section.

Statistical analysis

Data are presented as the mean values +/ī standard deviations from at least three independent experiments. Statistically significant differences between sample groups were determined using a Studentôs t-test with a p-valueÒ0.05 considered to be statistically significant (pÒ0.05 = *, pÒ 0.01 = **, pÒ0.001 = ***).

RESULTS

Strong utilization of the progerin and LAΔ35 5ôSSs in the *βGlo*-LMNA c.1822G>A and c.1868C>G transcripts

To compare the yield of utilization of the lamin A, progerin and LAΔ35 5ôSSs in the WT and mutated contexts, we used the previously described *βGlo*-LMNA minigene [Lopez-Mejia, et al., 2011] (Figure 2). In this minigene, the WT LMNA gene sequence extending from exons 11 through 12 had been cloned downstream from the β-globin intron 1 in the βglo3S

plasmid [Labourier et al., 1999]. By site-directed mutagenesis, we introduced each of the HGPS mutations in this construct. HeLa cells were transiently transfected with the WT or mutated β*Glo*-LMNA constructs and the effects of the mutations on exon 11 5ôSS utilization were tested by RT-PCR. To this end, we used two primers, which were respectively located on each side of the alternatively spliced regions, so that the size of the amplified products depended upon the identity of the 5ôSS used for intron 11 excision (Figure 2A). As a control, we generated the 1968+1 G>A β*Glo*-LMNA variant construct. This substitution was expected to destroy the lamin A 5ôSS. Accordingly, while only a main band, was obtained for the WT construct, corresponding to cDNA amplified from products spliced at the lamin A 5ôSS, a single amplified product with a 150 bp deletion corresponding to progerin 5ôSS utilization was obtained for the 1968+1G>A variant (Figure 2B-C, lanes 1 and 13). The same truncated cDNA product was also predominantly detected for each of the 1824C>T and 1822G>A *βGlo*-LMNA transcripts, indicating an almost complete splicing at the progerin 5ôSS in the corresponding pre-mRNAs, at the expense of the lamin A 5ôSS (Figure 2B-C, lanes 4 and 7 versus 1). In cells transfected with the 1868C>G *βGlo*-LMNA minigene, about half of the cDNA molecules detected corresponded to splicing at the lamin A 5ôSS, while the other half carried the 105 bp deletion generated by splicing at the LAΔ35 5ôSS (Figure 2B-C, lane 10). Such a high level of utilization of the progerin 5ôSS in the presence of the 1822G>A and 1824C>T nucleotide transitions, and of the LAΔ35 5ôSS in the presence of the 1868C>G nucleotide transversion, was not predicted by computer analysis, reinforcing the idea that the strong utilization of the progerin and LAΔ35 5ôSSs in the HGPS genetic contexts reflects regulatory mechanisms involving nuclear protein factors.

SRSF1 and SRSF5 overexpressions limit progerin and LAΔ35 5ôSSs utilization in HeLa cells

As SR proteins are major regulators of alternative splicing, and that we previously observed an effect of depletion of the SR proteins SRSF1 and SRSF6 on utilization of the progerin 5ôSS in the c.1824C>T context [Lopez-Mejia, et al., 2011], we decided to extend the analysis of the SRSF1 effect on the progerin 1822G>A and LAΔ35 1868C>G 5ôSSs. Furthermore, as preliminary data suggested a possible activity of the SR protein SRSF5 on splicing at the LMNA 5ôSS [Lopez-Mejia, et al., 2011], we also tested the effect of an overexpression of this protein on the utilization of intron 11 5ôSSs. To this end, pXJ41 plasmid derivatives allowing the overexpression of SRSF1 or SRSF5 were co-transfected in HeLa cells, with either the WT or one of the mutated *βGlo*-LMNA reporter constructs. The control cells were co-transfected with an empty pXJ41 vector. The level of SR protein overexpression was estimated by western blot analysis using dedicated antibodies (Supp. Figure S1A). The data obtained demonstrated that overexpression of SRSF5 or SRSF1 in HeLa cells greatly limits the use of the progerin 1824C>T, progerin 1822G>A and LAΔ35 1868C>G 5ôSSs, whereas utilization of the lamin A 5ôSS was increased in these three mutated contexts (Figure 2B-C, lanes 4-12).

To check whether the levels of overexpression of protein SRSF5 that we used in the above experiments were in a physiological range, we performed dose effect experiments. Increasing amounts (10, 50 and 250 ng) of the recombinant pXJ41- SRSF5, were co-transfected in HeLa cells, with either the 1824C>T, 1822G>A or the 1868C>G *βglo*-LMNA construct, and the impact on the relative rates of utilization of intron 11 5ôSSs was analyzed by RT-PCR. As a control, similar assays were performed with a pXJ41 plasmid expressing the SR protein SRSF7, which was not found to alter intron 11 5ôSS utilization in preliminary assays. A rather linear relationship was observed between the increased amount of transfected pXJ41-SRSF5 plasmid and the decreased use of the progerin and LAΔ35 5ôSS in the transcripts (Figure 2D). Similar results were obtained for SRSF1 (data not shown). In contrast, no significant variations

of the relative utilizations of intron 11 5ôSSs were observed when using plasmid pXJ41-SRSF7, confirming the absence of activity of SRSF7 on these 5ôSSs (Figure 2D). Altogether, we concluded that both SRSF5 and SRSF1, but not SRSF7, have a modulating activity on the utilization of the alternative 5ôSSs of intron 11.

Importantly, SRSF1 and SRSF5 did not abolish or reduce the utilization of the progerin or LAΔ35 5ôSSs in pre-mRNAs containing the 1968+1G>A mutation that killed the lamin A 5ôSS. This suggests that the effect observed in the presence of an active lamin A 5ôSS corresponds to its activation by SR proteins (Figure 2B-C lane 13-15 and Supp. Figure S1B). However, these *in cellulo* assays were not sufficient to determine whether SRSF1 and SRSF5 have a direct effect on selection of the intron 11 5ôSSs or an indirect effect resulting from a complex cascade of events. Therefore, to get more information on the SRSF1 and SRSF5 activities on selection of intron 11 5ôSSs, we turned to *in vitro* splicing assays.

In vitro splicing assays confirm the direct effect of SRSF5 on intron 11 5ôSS selection

To determine whether SRSF1 and SRSF5 have a direct effect on intron 11 5ôSS selection, we took advantage of the possibility to use the *βGlo*-LMNA minigene for both *in cellulo* and *in vitro* splicing assays [Lopez-Mejia, et al., 2011]. As observed in Figure 3, after 2 hours of incubation in a nuclear extract or in a time scale study (Supp. Figure S2), *in vitro* splicing in HeLa cells nuclear extract of the 1822G>A *βglo*-LMNA pre-mRNA produced mRNAs arising from the utilization of both the lamin A and progerin 5ôSSs, with a predominant use of the progerin 5ôSS (Figure 3A lane 1 and Supp. Figure S2B, lanes 8-13 and 2C). The splicing pattern observed for the 1868C>G *βglo*-LMNA pre-mRNA was more complex, since the lamin A, LAΔ35 and also the progerin 5SSs were used (Figure 3A lane 8 and Supp. Figure S2B, lanes 15-20 and S2C), and the yield of utilization of the progerin 5ôSS was quite similar

to that observed for the WT *βglo*-LMNA pre-mRNA (Figure 3A and compare lanes 1-6 and 15-20 in Supp. Figure S2B), confirming that the progerin 5ôSS is an authentic alternative 5ôSS.

The effects of proteins SRSF1 and SRSF5 on the splicing patterns of the WT, 1824C>T, 1822G>A and 1868C>G *βglo*-LMNA pre-mRNAs were then tested by addition of increasing amounts (200 and 400 ng) of recombinant SR proteins to the nuclear extract. When using the WT *βglo*-LMNA pre-mRNAs as the substrate, addition of recombinant SRSF1 led to an increased utilization of the lamin A 5ôSS at the expense of the progerin 5ôSS (Figure 3A, compare lane 5 with lanes 6-7 and see quantifications). As previously observed for the 1824C>T *βglo*-LMNA substrate [Lopez-Mejia, et al., 2011], when using the 1822G>A *βglo*-LMNA transcript, an increased utilization of the lamin A 5ôSS with a parallel decrease of the progerin 5ôSSs was observed upon addition of SRSF1 (Figure 3B). A complete inversion of the relative use of the progerin and lamin A 5ôSSs was observed at the highest SRSF1 concentration (Figure 3A, compare lane 1 with lanes 2-3 and see quantifications). In contrast, although production of the progerin mRNA from the 1868C>G *βglo*-LMNA transcript was decreased upon addition of SRSF1, the rate of utilization of the LAΔ35 5ôSS was mostly unaffected (Figure 3A, compare lane 8 with lanes 9-10 and see quantifications). Taken together, the data shows that *in vitro*, SRSF1 directly regulates the relative use of the lamin A and progerin 5ôSSs, but has no effect on the LAΔ35 5ôSS utilization.

As shown in Figure 3B, an increased concentration of SRSF5 also markedly increased the lamin A 5ôSS utilization at the expense of the progerin 5ôSS utilization in the WT, 1824 C>T and 1822 G>A *βglo*-LMNA transcripts. Interestingly, at the highest concentration, in contrast to SRSF1, SRSF5 abolished the use of the LAΔ35 5ôSS in the 1868 C>G *βglo*-LMNA pre-mRNA and all the tested transcripts were almost exclusively processed at the lamin A 5ôSS (Figure 3B, compare lane 1 to 2-3, lane 4 to 5-6, lane 7 to 8-9 and lane 10 to 11-12). SRSF5 also slightly increased the global splicing efficiency, since more double-spliced RNA species

were produced compared to controls. Taken together, the data obtained show that in *in vitro* assays, SRSF5 directly modulates the relative yields of utilization of the progerin, LAΔ35 and lamin A 5′SSs of LMNA intron 11.

Enhanced SRSF5 expression decreases progerin 5′SS utilization in fibroblasts of a HGPS patient.

Our finding that SRSF5 favors the lamin A 5′SS utilization at the expense of both the progerin and the LAΔ35 5′SSs in HeLa cells transfected with the *βGlo*-LMNA construct was attractive in terms of potential HGPS therapy. However, the relative concentration and activity of SR proteins are known to depend upon the cellular context [Fu and Ares, 2014]. Hence, to confirm the relevance of our observation, we had to firstly check whether the observed regulation is also found in other cell lines, and secondly to verify that the SRSF5 activity discovered by using the *βGlo*-LMNA minigene transcript reflected an authentic regulation of the endogenous LMNA transcript. As dermal primary cells of a patient bearing the c.1824C>T mutation were available, we thought that it would be interesting to use primary culture of human dermal fibroblasts for these control assays.

First, we performed transitory transfection of human dermal fibroblasts from a healthy patient with the *βGlo*-LMNA minigenes. The relative yields of utilization of the lamin A and progerin 5′SSs were found to be very similar in fibroblasts compared to HeLa cells, and a similar increase of the lamin A 5′SS utilization at the expense of the progerin 5′SS usage was observed upon SRSF1 or SRSF5 overexpression (data not shown). This encouraged us to compare the splicing regulation of the endogenous LMNA gene in fibroblasts isolated from this healthy patient and in fibroblasts from the HGPS patient bearing the c.1824C>T mutation. To increase the intracellular SRSF5 concentration, plasmid pXJ41-SRSF5 was transfected into the fibroblast cells by nucleofection. The SRSF5 overexpression was tested by Western Blot

analysis (Figure 4A). The identity and yield of intron 11 5ô SS utilization was analyzed by RTï PCR using primers located in exons 8 and 12, respectively. Consistent with the results obtained *in vitro* and in HeLa cells, SRSF5 overexpression in fibroblasts of the HGPS patient slightly but significantly increased the use of the endogenous lamin A 5NSS, with a concomitant decrease of the progerin 5NSS utilization (Fig. 4B). The low yield of cell transfection (about 40 % as estimated by flow cytometry) might have participated to our finding of only a moderate change in intron 11 5ô SS utilization.

PDGF-BB stimulation decreases progerin 5NSS utilization in fibroblasts of a HGPS patient and improves nuclear morphology

To try to overcome these transfection limitations, we looked for another possible strategy to enhance SRSF5 activity in HGPS cells. Several reports had highlighted the ability of growth factor (PDGF-BB, EGF or TGFβ) or PIK3/Akt stimulation to mediate alternative splice-site selection by changing the phosphorylation status of hnRNPs and SR proteins. In particular, activation of SRSF5 through its phosphorylation via Akt activation had been proposed [Patel et al., 2005; Blaustein et al., 2005]. To test for the impact of an enhanced SRSF5 activity on endogenous LMNA intron 11 splicing, we stimulated HGPS dermal fibroblasts with 20 ng/ml of PDGF-BB for 24 hours. As expected, PDGF-BB stimulation of HGPS dermal fibroblasts led to Akt phosphorylation and to a medium, but significant increase of the level of phosphorylated SRSF5 (Supp. Figure S3A). Some increase of SRSF1 and/or SRSF2 and SRSF6 phosphorylation was also observed, whereas SRSF4 and 7 were almost unaffected (Supp. Figure S3A). Interestingly, the stimulation of HGPS dermal fibroblasts with PDGF-BB amounts ranging from 10 to 160 ng/ml for 24 hours revealed a dose-dependent increased usage of the endogenous lamin A 5NSS with a concomitant decrease of the progerin 5NSS utilization (Supp. Figure S3B). The impact of PDGF-BB stimulation was further characterized using the

40 ng/ml dose, leading to stronger splicing improvement compared to the 20 ng/ml dose used above. Moreover, in order to be able to detect a PDGF-BB impact on the expression level of progerin, which has a half-life of about 24 hours, the time frame of the stimulation was changed from 24 hours to 4 days with a daily administration [Cao et al., 2011]. In these experimental conditions, PDGF-BB stimulation of HGPS dermal fibroblasts led to a 30 % reduction of the progerin/lamin A ratio originated from an increase of the lamin A mRNA and protein level. (Figure 5A and 5B). We next tested whether this PDGF-BB treatment resulted in some recovery of the nuclear membrane structure. To this goal, changes in nuclear dysmorphic features (lobulations, herniations or folding of the nuclear envelope) upon PDGF treatment were estimated as described in Materials and Methods. Whereas mean values for dysmorphic nuclei of 49 % and 9% were established for mock treated HGPS fibroblasts and control fibroblasts, these means were respectively reduced to 28 and 5 % after PDGF treatment (Figure 5C and 5D). This positive impact of the PDGF-BB stimulation on nuclear membrane shape was further confirmed by automated measurement of nuclei morphometric parameters, such as solidity and aspect ratio using the Image J software (Supp. Methods). Solidity (area divided by convex area) provides a sense of the nuclei irregularity. It is equal to 1 for nuclei with no invagination (convex) and it decreases as nuclei become more lobulated (Choi et al., 2011; Booth-Gauthier et al., 2013). Accordingly, the average solidity of multilobed HGPS fibroblast nuclei (0.9817 ± 0.0011) was significantly smaller than that of control fibroblasts (0.9916 ± 0.0002; p-value = 1.76E-15). Upon treatment with PDGF-BB, HGPS cells presented with a significant increase of their average solidity (0.9861 ± 0.0005; p-value = 8.13E-04) indicating that their nuclei became more solid and regular (Figure 5E). Aspect ratio (major axis divided by minor axis) evaluates the shape and more especially the elongation of the nuclei. According to literature, HGPS nuclei show a more circular overall shape since the micro-dysmorphic shapes prevents proper elongation of nuclei (Choi et al., 2011; Booth-Gauthier et al., 2013; Barthelemy, et al.,

2015). Accordingly, in our experiments, control fibroblasts nuclei were found to be more ovoid than HGPS nuclei (nuclei aspect ratio of 1.49 ± 0.01 against 1.30 ± 0.01; p-value = 1.52E-19). The significant increase of the average aspect ratio of HGPS nuclei (1.40 ± 0.01; p-value = 2.06E-07) observed upon PDGF-BB treatment indicated a significant improvement of their morphology (Figure 5C and 5E).

Although, we could not identify which of the phosphorylated protein(s) was/were responsible for the observed modification of alternative splicing in these experiments, the data obtained demonstrated that phosphorylation of some of the SR proteins, including SRSF5, can partially correct the intron 11 splicing defect in fibroblast of HGPS patients, and thus reduce the progerin/Lamin A ratio and improve the morphology of HGPS nuclei.

DISCUSSION

All three known HGPS causing mutations (c.1824C>T, c.1822G>A and c.1868C>G) affect splicing of the LMNA exon 11, leading to generation of partially processed and truncated lamin A proteins whose toxicity is mainly due to the presence of a residual farnesylated modification anchoring them at the plasma membrane. Therefore, strategies for progeria treatments were oriented either towards limitation of the farnesylation of the partially processed protein, or towards limitation of their production by restoration of normal splicing. Although, limiting farnesylation of the un-completely processed protein has been tested for a while, there are still limitation in the clinical utilization of this therapy. Farnesyltransferase inhibitors (FTI) successfully limit HGPS negative effects in cell culture, animal models and HGPS patients [Meta et al., 2006; Yang et al., 2008; Gordon et al., 2012; Ullrich et al., 2013]. However, FTI administration results in the activation of a geranylgeranylation site in prelamin A. To prevent production of both farnesyl and geranylgeranyl precursors, FTIs have been combined with pravastatin (a statin) and zoledronic acid (an aminobisphosphonate) [Varela et al., 2008].

Nevertheless, recent studies established that FTase deficiency leads to severe alopecia and is associated with apoptosis of keratinocytes revealing potent risks of FTI-based therapies [Davies et al., 2010; Le Dour et al., 2011; Lee et al., 2010].

Oligonucleotide based therapeutic strategies have also been designed in order to restore lamin A expression. For instance, the HGPS phenotype was found to be successfully reversed by treatment with an antisense morpholino oligonucleotide targeting the progerin 5ôSS in a HGPS mouse model. Inhibition of the progerin 5ôSS resulted in improved body weight, extended lifespan, and correction of several of the deleterious phenotypes [Scaffidi and Misteli, 2005; Osorio et al., 2011]. Progerin mRNA expression levels were also successfully decreased by using siRNA-based methods [Huang et al., 2005]. However, systemic delivery of oligonucleotides and siRNAs in human remains a challenge. Therefore, the possibility to reinforce the utilization of the laminA 5ôSS by the use of simple chemical molecules, in particular activators of SR proteins, still remains of high interest. This has strengthened our interest to improve our knowledge on how alternative splicing of LMNA intron 11 is regulated. In a previous study, we had already started to decipher the mechanisms accounting for splice site selection in the presence of the prominent c.1824C>T mutation, and we identified the SR proteins SRSF1 and SRSF6 as modulators of the utilization of the LMNA and progerin 5ôSSs [Lopez-Mejia, et al., 2011]. Here, we completed this investigation by studying the effect of SRSF5 and extended it to the two other HGPS mutations.

First of all, in agreement with computational analyses, our *in vitro* studies confirm that the progerin 5ôSS is recognized in nuclear extract as an authentic 5ôSS, even in the absence of HGPS mutations. The HGPS mutations just increase its yield of utilization. Therefore, progerin is probably expressed at low level in most of the human cells, suggesting that it may be of functional importance. In agreement with this hypothesis, recent data obtained by studying metabolism in mice [Lopez-Mejia et al., 2014] revealed antagonist functions of lamin C and

progerin in energy metabolisms, so that a moderate progerin expression in normal cells may partially counteract the property of lamin C to reduce energy metabolism.

Secondly, in contrast to the progerin 5ôSS, the LAΔ35 5ôSS is not used in a WT context. It is only used in the presence of the 1868C>G mutation, confirming that this 5ôSS is created *de novo* by the mutation. In addition, our *in cellulo* experiments using HeLa cells and the ***b****Glo*-LMNA reporter gene show that in the presence of the 1868C>G mutation, utilization of the LAΔ35 5ôSS site does not abrogate completely the utilization of the LMNA 5ôSS. This may explain the longer life of the unique HGPS patient characterized with this mutation. He survived to age 45, while the patients bearing the 1824C>T and 1822G>A transitions have shorter life spans (most patients die by age 13). Fukuchi and colleagues [Fukuchi, et al., 2004], who identified the 1868C>G HSPG mutation, considered that the associated longer life span might reflect less harmful property of the 35 amino acid truncation in LAΔ35 compared to the 50 amino acid truncation in progerin. However, both progerin and LAΔ35 retain the CAAX farnesylation site and lack the endo-proteolytic cleavage site, which seem to be key determinants of the pathology. Therefore, based on the present data, we hypothesize that the longer life span of the patient carrying the 1868C>G transversion was at least in part due to a lower yield of expression of LAΔ35 protein as compared to progerin production in the presence of the 1824C>T or 1822G>A transition. This hypothesis is also in agreement with previous results showing that in the presence of the 1868C>G mutation about 80% of the LMNA mRNA correspond to full length lamin A mRNA, against only 15.5% in the presence of the 1824C>T mutation [Fukuchi, et al., 2004; Reddel and Weiss, 2004]. Accordingly, improving the production of lamin A mRNA in patients carrying the 1824C>T and 1822G>A mutations at a level similar to that found in the patient with the 1868C>G mutation might extend their life span up to 40-50 years.

Third, in line with this goal, our identification of a new player, the SR protein SRSF5, in the regulation of the utilization of the LMNA 5ôSS versus the progerin or LAΔ35 5ôSS, and our observation of the activation of the LMNA 5ôSS by PDGF-BB treatment are promising discoveries in the perspective to develop new therapy. Interestingly, while increased expressions of SRSF1 and SRSF5 in HeLa cells both increased the yield of utilization of the LMNA 5ôSS at the expense of the progerin and the LAΔ35 5ôSSs, the positive effect on LMNA 5ôSS utilization resulting from addition of the SRSF5 or SRSF1 recombinant protein in a HeLa cell nuclear extract depends upon the type of HGPS mutation. The absence of increase of LMNA 5ôSS utilization upon SRSF1 addition in the presence of the 1868C>G mutation and the fact that high amounts of SRSF1 should be added to get a significant increase of the utilization of this 5ôSS in the presence of the two other HGPS mutations suggest that SRSF1 has a complex effect on LMNA intron 11 splicing. Therefore, in the perspective to limit HGPS defects linked to different LMNA mutations, increasing SRSF5 activity seems more powerful than increasing SRSF1 activity.

SRSF5 is very interesting for this purpose, as we show that increasing its expression in dermal fibroblasts cells isolated from a HGPS patient decreases the use of the progerin 5ôSS. Our results may explain data from Fong et al. [Fong et al., 2009]. These authors searched for antisense oligonucleotides that may reinforce the production of progerin transcripts in both WT and HGPS fibroblasts. They identified 2 overlapping anti-sense oligonucleotides, ASO 074 and 324, targeting a 25 nucleotide region (nucleotide positions 1852 to 1869 for ASO 074 and 1857 to 1875 for ASO 324). This region is located roughly 100 nucleotides upstream of the lamin A 5ôSS and 40-50 nucleotides downstream from the progerin 5'SS. It contains nucleotide sequences (UCACTCG, GCAGC and ACCGC) which are identified as putative SRSF5 binding sites by ESE Finder (http://rulai.cshl.edu/tools/ESE2/index.html) and SpliceAid (http://www.introni.it/splicing.html) softwares. This region might therefore contain the exonic

splicing enhancer (ESE) responsible for the SRSF5 activation effect that we detected. In addition, more recently, Luo and colleagues developed splice-switching oligonucleotides to redirect splicing of LMNA transcripts in order to produce a model of accelerated muscle ageing in human myogenic cells [Luo et al., 2014]. Interestingly the identified oligonucleotides showing the highest splice switching properties cover either a region located 30 to 50 nts upstream of the lamina 5ôSS, or the 25 nt segment containing the putative SRSF5 ESE, reinforcing the idea that SRSF5 may be a key player in the control of progerin production. The sequences identified in the studies by both Fong et al. and Luo et al. may also contain SRSF1 or SRSF6 ESEs as these two proteins both activate the LMNA 5ôSS utilization [Lopez-Mejia, et al., 2011]. Interestingly, PDGF-BB stimulation of HGPS fibroblasts likely activates the three proteins able to increase the LMNA 5ôSS utilization at the expense of the progerin and LAΔ35 5ôSS utilization, since an increased phosphorylation of SRSF1, SRSF5 and SRSF6 was detected after the stimulation. The observation of partial splicing recovery, reduced progerin/lamin A ratio and the improvement of HGPS nuclei morphology upon PDGF-BB stimulation represents a highly promising perspective in the view to design new HGPS treatment. Importantly, the use of recombinant human PDGF-BB has been evaluated for potential toxicity in a variety of studies without observation of toxicity, carcinogenicity, or mutagenicity even at concentration higher than 1 µg/ml. This suggests that while PDGF-BB stimulation affects LMNA exon 11 splicing regulation it does not have deleterious effect on the cells due to massive changes in global splicing regulation (Solchaga et al., 2012). Owing to this absence of toxicity, PDGF-BB is already FDA-approved for use in the treatment of localized periodontal defects and disabetic ulcers [Jin et al., 2004; Nevins et al., 2005; Uhl et al., 2003; Simion et al., 2008], and PDGF-based therapies are currently developed for the treatment of several diseases including myocardial infarction, skeletal disorders and chronic wound healing [Cui et al., 2014; Chang et al., 2010]. Nevertheless, in the case of HGPS, while PDGF-BB treatment appears effective at

improving nuclear shape abnormalities of HGPS fibroblasts, it has remained to be demonstrated whether normalization of nuclear morphology translates into a general rescue of cellular function and the reversal of HGPS tissue-specific phenotypes.

ACKNOWLEDGEMENTS

V.V. was supported by a graduate fellowship from the Ministère Délégué à la Recherche et aux Technologies and a 4th year PhD fellowship by the Fondation pour la Recherche Médicale (FRM, FDT20120925471). This work was funded by CNRS and Lorraine university (UMR 7365 and 7114) and the international LIA laboratory N°546 on alternative splicing, by grants from the Agence Nationale de la Recherche (ANR-05-BLAN-0261-01) and the European Alternative Splicing Network of Excellence (EURASNET, FP6 life sciences, genomics and biotechnology for health) and Région Lorraine (PRST IMTS). C. Weldon is thanked for improving the use of English in the manuscript.

CONFLICT OF INTEREST STATEMENT

None declared.

REFERENCES

Barthelemy F, Navarro C, Fayek R, Da Silva N, Roll P, Sigaudy S, Oshima J, Bonne G, Papadopoulou-Legbelou K, Evangeliou AE, Spilioti M, Lemerrer M, et al. 2015. Truncated prelamin A expression in HGPS-like patients: a transcriptional study. Eur J Hum Genet.

Black DL 2003. Mechanisms of alternative pre-messenger RNA splicing. Annu Rev Biochem 72: 291-336.

Blaustein M, Pelisch F, Tanos T, Munoz MJ, Wengier D, Quadrana L, Sanford JR, Muschietti JP, Kornblihtt AR, Caceres JF, Coso OA, Srebrow A 2005. Concerted regulation of nuclear and cytoplasmic activities of SR proteins by AKT. Nat Struct Mol Biol 12: 1037-1044.

Booth-Gauthier EA, Du V, Ghibaudo M, Rape AD, Dahl KN, Ladoux B 2013. Hutchinson-Gilford progeria syndrome alters nuclear shape and reduces cell motility in three dimensional model substrates. Integr Biol (Camb) 5: 569-577.

Bourgeois CF, Lejeune F, Stevenin J 2004. Broad specificity of SR (serine/arginine) proteins in the regulation of alternative splicing of pre-messenger RNA. Prog Nucleic Acid Res Mol Biol 78: 37-88.

Cao K, Capell BC, Erdos MR, Djabali K, Collins FS 2007. A lamin A protein isoform overexpressed in Hutchinson-Gilford progeria syndrome interferes with mitosis in progeria and normal cells. Proc Natl Acad Sci U S A 104: 4949-4954.

Cao K, Graziotto JJ, Blair CD, Mazzulli JR, Erdos MR, Krainc D, Collins FS 2011. Rapamycin reverses cellular phenotypes and enhances mutant protein clearance in Hutchinson-Gilford progeria syndrome cells. Sci Transl Med 3: 89ra58.

Cavaloc Y, Bourgeois CF, Kister L, Stevenin J 1999. The splicing factors 9G8 and SRp20 transactivate splicing through different and specific enhancers. RNA 5: 468-483.

Chang PC, Seol YJ, Cirelli JA, Pellegrini G, Jin Q, Franco LM, Goldstein SA, Chandler LA, Sosnowski B, Giannobile WV 2010. PDGF-B gene therapy accelerates bone engineering and oral implant osseointegration. Gene Ther 17: 95-104.

Choi S, Wang W, Ribeiro AJ, Kalinowski A, Gregg SQ, Opresko PL, Niedernhofer LJ, Rohde GK, Dahl KN 2011. Computational image analysis of nuclear morphology associated with various nuclear-specific aging disorders. Nucleus 2: 570-579.

Cui Y, Sun YW, Lin HS, Su WM, Fang Y, Zhao Y, Wei XQ, Qin YH, Kohama K, Gao Y 2014. Platelet-derived growth factor-BB induces matrix metalloproteinase-2 expression and rat

vascular smooth muscle cell migration via ROCK and ERK/p38 MAPK pathways. Mol Cell Biochem 393: 255-263.

Davies BS, Barnes RH, 2nd, Tu Y, Ren S, Andres DA, Spielmann HP, Lammerding J, Wang Y, Young SG, Fong LG 2010. An accumulation of non-farnesylated prelamin A causes cardiomyopathy but not progeria. Hum Mol Genet 19: 2682-2694.

De Sandre-Giovannoli A, Bernard R, Cau P, Navarro C, Amiel J, Boccaccio I, Lyonnet S, Stewart CL, Munnich A, Le Merrer M, Levy N 2003. Lamin a truncation in Hutchinson-Gilford progeria. Science 300: 2055.

Dechat T, Shimi T, Adam SA, Rusinol AE, Andres DA, Spielmann HP, Sinensky MS, Goldman RD 2007. Alterations in mitosis and cell cycle progression caused by a mutant lamin A known to accelerate human aging. Proc Natl Acad Sci U S A 104: 4955-4960.

Eriksson M, Brown WT, Gordon LB, Glynn MW, Singer J, Scott L, Erdos MR, Robbins CM, Moses TY, Berglund P, Dutra A, Pak E, et al. 2003. Recurrent de novo point mutations in lamin A cause Hutchinson-Gilford progeria syndrome. Nature 423: 293-298.

Faustino NA, Cooper TA 2003. Pre-mRNA splicing and human disease. Genes Dev 17: 419-437.

Fong LG, Vickers TA, Farber EA, Choi C, Yun UJ, Hu Y, Yang SH, Coffinier C, Lee R, Yin L, Davies BS, Andres DA, et al. 2009. Activating the synthesis of progerin, the mutant prelamin A in Hutchinson-Gilford progeria syndrome, with antisense oligonucleotides. Hum Mol Genet 18: 2462-2471.

Fu XD, Ares M, Jr. 2014. Context-dependent control of alternative splicing by RNA-binding proteins. Nat Rev Genet 15: 689-701.

Fukuchi K, Katsuya T, Sugimoto K, Kuremura M, Kim HD, Li L, Ogihara T 2004. LMNA mutation in a 45 year old Japanese subject with Hutchinson-Gilford progeria syndrome. J Med Genet 41: e67.

Gamazon ER, Stranger BE 2014. Genomics of alternative splicing: evolution, development and pathophysiology. Hum Genet 133: 679-687.

Glynn MW, Glover TW 2005. Incomplete processing of mutant lamin A in Hutchinson-Gilford progeria leads to nuclear abnormalities, which are reversed by farnesyltransferase inhibition. Hum Mol Genet 14: 2959-2969.

Goldberg M, Harel A, Gruenbaum Y 1999. The nuclear lamina: molecular organization and interaction with chromatin. Crit Rev Eukaryot Gene Expr 9: 285-293.

Gordon LB, Kleinman ME, Miller DT, Neuberg DS, Giobbie-Hurder A, Gerhard-Herman M, Smoot LB, Gordon CM, Cleveland R, Snyder BD, Fligor B, Bishop WR, et al. 2012. Clinical trial of a farnesyltransferase inhibitor in children with Hutchinson-Gilford progeria syndrome. Proc Natl Acad Sci U S A 109: 16666-16671.

Hisama FM, Lessel D, Leistritz D, Friedrich K, McBride KL, Pastore MT, Gottesman GS, Saha B, Martin GM, Kubisch C, Oshima J 2011. Coronary artery disease in a Werner syndrome-like form of progeria characterized by low levels of progerin, a splice variant of lamin A. Am J Med Genet A 155A: 3002-3006.

Huang S, Chen L, Libina N, Janes J, Martin GM, Campisi J, Oshima J 2005. Correction of cellular phenotypes of Hutchinson-Gilford Progeria cells by RNA interference. Hum Genet 118: 444-450.

Jin Q, Anusaksathien O, Webb SA, Printz MA, Giannobile WV 2004. Engineering of tooth-supporting structures by delivery of PDGF gene therapy vectors. Mol Ther 9: 519-526.

Labourier E, Allemand E, Brand S, Fostier M, Tazi J, Bourbon HM 1999. Recognition of exonic splicing enhancer sequences by the Drosophila splicing repressor RSF1. Nucleic Acids Res 27: 2377-2386.

Le Dour C, Schneebeli S, Bakiri F, Darcel F, Jacquemont ML, Maubert MA, Auclair M, Jeziorowska D, Reznik Y, Bereziat V, Capeau J, Lascols O, et al. 2011. A homozygous

mutation of prelamin-A preventing its farnesylation and maturation leads to a severe lipodystrophic phenotype: new insights into the pathogenicity of nonfarnesylated prelamin-A. J Clin Endocrinol Metab 96: E856-862.

Lee R, Chang SY, Trinh H, Tu Y, White AC, Davies BS, Bergo MO, Fong LG, Lowry WE, Young SG 2010. Genetic studies on the functional relevance of the protein prenyltransferases in skin keratinocytes. Hum Mol Genet 19: 1603-1617.

Lopez-Mejia IC, de Toledo M, Chavey C, Lapasset L, Cavelier P, Lopez-Herrera C, Chebli K, Fort P, Beranger G, Fajas L, Amri EZ, Casas F, et al. 2014. Antagonistic functions of LMNA isoforms in energy expenditure and lifespan. EMBO Rep 15: 529-539.

Lopez-Mejia IC, Vautrot V, De Toledo M, Behm-Ansmant I, Bourgeois CF, Navarro CL, Osorio FG, Freije JM, Stevenin J, De Sandre-Giovannoli A, Lopez-Otin C, Levy N, et al. 2011. A conserved splicing mechanism of the LMNA gene controls premature aging. Hum Mol Genet 20: 4540-4555.

Luo YB, Mitrpant C, Adams AM, Johnsen RD, Fletcher S, Mastaglia FL, Wilton SD 2014. Antisense oligonucleotide induction of progerin in human myogenic cells. PLoS One 9: e98306.

Meta M, Yang SH, Bergo MO, Fong LG, Young SG 2006. Protein farnesyltransferase inhibitors and progeria. Trends Mol Med 12: 480-487.

Moulson CL, Fong LG, Gardner JM, Farber EA, Go G, Passariello A, Grange DK, Young SG, Miner JH 2007. Increased progerin expression associated with unusual LMNA mutations causes severe progeroid syndromes. Hum Mutat 28: 882-889.

Naro C, Sette C 2013. Phosphorylation-mediated regulation of alternative splicing in cancer. Int J Cell Biol 2013: 151839.

Navarro CL, De Sandre-Giovannoli A, Bernard R, Boccaccio I, Boyer A, Genevieve D, Hadj-Rabia S, Gaudy-Marqueste C, Smitt HS, Vabres P, Faivre L, Verloes A, et al. 2004. Lamin A

and ZMPSTE24 (FACE-1) defects cause nuclear disorganization and identify restrictive dermopathy as a lethal neonatal laminopathy. Hum Mol Genet 13: 2493-2503.

Nevins M, Giannobile WV, McGuire MK, Kao RT, Mellonig JT, Hinrichs JE, McAllister BS, Murphy KS, McClain PK, Nevins ML, Paquette DW, Han TJ, et al. 2005. Platelet-derived growth factor stimulates bone fill and rate of attachment level gain: results of a large multicenter randomized controlled trial. J Periodontol 76: 2205-2215.

Osorio FG, Navarro CL, Cadinanos J, Lopez-Mejia IC, Quiros PM, Bartoli C, Rivera J, Tazi J, Guzman G, Varela I, Depetris D, de Carlos F, et al. 2011. Splicing-directed therapy in a new mouse model of human accelerated aging. Sci Transl Med 3: 106ra107.

Patel NA, Kaneko S, Apostolatos HS, Bae SS, Watson JE, Davidowitz K, Chappell DS, Birnbaum MJ, Cheng JQ, Cooper DR 2005. Molecular and genetic studies imply Akt-mediated signaling promotes protein kinase CbetaII alternative splicing via phosphorylation of serine/arginine-rich splicing factor SRp40. J Biol Chem 280: 14302-14309.

Reddel CJ, Weiss AS 2004. Lamin A expression levels are unperturbed at the normal and mutant alleles but display partial splice site selection in Hutchinson-Gilford progeria syndrome. J Med Genet 41: 715-717.

Ropers D, Ayadi L, Gattoni R, Jacquenet S, Damier L, Branlant C, Stevenin J 2004. Differential effects of the SR proteins 9G8, SC35, ASF/SF2, and SRp40 on the utilization of the A1 to A5 splicing sites of HIV-1 RNA. J Biol Chem 279: 29963-29973.

Scaffidi P, Misteli T 2005. Reversal of the cellular phenotype in the premature aging disease Hutchinson-Gilford progeria syndrome. Nat Med 11: 440-445.

Scaffidi P, Misteli T 2006. Lamin A-dependent nuclear defects in human aging. Science 312: 1059-1063.

Scaffidi P, Misteli T 2008. Lamin A-dependent misregulation of adult stem cells associated with accelerated ageing. Nat Cell Biol 10: 452-459.

Shalev SA, De Sandre-Giovannoli A, Shani AA, Levy N 2007. An association of Hutchinson-Gilford progeria and malignancy. Am J Med Genet A 143A: 1821-1826.

Shumaker DK, Dechat T, Kohlmaier A, Adam SA, Bozovsky MR, Erdos MR, Eriksson M, Goldman AE, Khuon S, Collins FS, Jenuwein T, Goldman RD 2006. Mutant nuclear lamin A leads to progressive alterations of epigenetic control in premature aging. Proc Natl Acad Sci U S A 103: 8703-8708.

Simion M, Rocchietta I, Monforte M, Maschera E 2008. Three-dimensional alveolar bone reconstruction with a combination of recombinant human platelet-derived growth factor BB and guided bone regeneration: a case report. Int J Periodontics Restorative Dent 28: 239-243.

Tazi J, Bakkour N, Marchand V, Ayadi L, Aboufirassi A, Branlant C 2010. Alternative splicing: regulation of HIV-1 multiplication as a target for therapeutic action. FEBS J 277: 867-876.

Uhl E, Rosken F, Sirsjo A, Messmer K 2003. Influence of platelet-derived growth factor on microcirculation during normal and impaired wound healing. Wound Repair Regen 11: 361-367.

Ullrich NJ, Kieran MW, Miller DT, Gordon LB, Cho YJ, Silvera VM, Giobbie-Hurder A, Neuberg D, Kleinman ME 2013. Neurologic features of Hutchinson-Gilford progeria syndrome after lonafarnib treatment. Neurology 81: 427-430.

Varela I, Pereira S, Ugalde AP, Navarro CL, Suarez MF, Cau P, Cadinanos J, Osorio FG, Foray N, Cobo J, de Carlos F, Levy N, et al. 2008. Combined treatment with statins and aminobisphosphonates extends longevity in a mouse model of human premature aging. Nat Med 14: 767-772.

Wahl MC, Will CL, Luhrmann R 2009. The spliceosome: design principles of a dynamic RNP machine. Cell 136: 701-718.

Wee CD, Havens MA, Jodelka FM, Hastings ML 2014. Targeting SR proteins improves SMN expression in spinal muscular atrophy cells. PLoS One 9: e115205.

Will CL, Luhrmann R 2001. Spliceosomal UsnRNP biogenesis, structure and function. Curr Opin Cell Biol. 13: 290-301.

Yang SH, Qiao X, Fong LG, Young SG 2008. Treatment with a farnesyltransferase inhibitor improves survival in mice with a Hutchinson-Gilford progeria syndrome mutation. Biochim Biophys Acta 1781: 36-39.

FIGURE LEGENDS

Figure 1: HGPS-associated mutations increase the predicted efficiencies of LMNA intron 11 alternative 5ôSSs.

(A) Organization of the primary transcripts of the LMNA gene in the WT and HGPS contexts: The most common HGPS-associated mutation, c.1824C>T, induces the exclusion of 150 nts from exon 11 resulting in the production of progerin, (protein LAΔ50). The c.1822G>A mutation activates the same alternative 5ô SS of intron 11 (progerin 5ôSS). The c.1968+1G>A mutation invalidates exon 11 lamin A 5ôSS and also activates the use of the progerin 5ôSS. A smaller C-terminal deletion in lamin A (35 amino acids, LAΔ35) resulting from *de novo* creation of a new LAΔ35 5ôSS in exon 11 was found to be associated with the c.1868C>G mutation. **(B)** Score calculations performed with MaxEntScan (MES) (http://genes.mit.edu.gate1.inist.fr/burgelab/maxent/Xmaxentscan_scoreseq.html), Splice-Site Analyzer Tool (SSAT) (http://ibis.tau.ac.il/ssat/SpliceSiteFrame.html) and Splice Site Score Calculation (http://rulai.cshl.edu/new_alt_exon_db2/HTML/score.html) [Shapiro and Senapathy, 1987; Yeo and Burge, 2004] indicate that the LMNA c1824C>T and c1822G>A mutations increase the score of the progerin 5ôSS, and the c.1868C>G mutation creates the LAΔ35 5ôSS (see Supp Methods section for details on the used algorithms). The sequences of the 5ôSSs are given together with the calculated scores. Nucleotide sequence differences as compared to the vertebrateôs consensus 5ôSS sequence are in bold. For each of the methods

used, the effects on scores of nucleotide sequence differences in the 5'SS as compared to the vertebrateôs consensus 5ôSS sequence are illustrated by ratios between scores obtained for the various WT and mutated exon 11 5' SSs versus the scores for the vertebrate's consensus 5'SS.

Figure 2: *In cellulo* activation of the LMNA 5ôSSs by SRSF1 and SRSF5.

(A) Schematic representation of constructs and primers used to test the effect of SR protein overexpression on utilization of the intron 11 5ôSSs. The primers used for RT-PCR analysis of splicing products are represented by horizontal arrows on schematized splicing products. The length in bps of the amplified DNA fragments corresponding to the utilization of the LMNA, progerin and LAΔ35 5ôSSs are given on the right. **(B)** Analysis of the effects of overexpression of SRSF1 and SRSF5 on intron 11 5ôSS utilization in WT and mutated *βglo* LMNA transcripts. The minigenes were co-transfected into HeLa cells together with the control empty pXJ41, or recombinant pXJ41-SRSF1 or pXJ41-SRSF5 plasmids. Efficiencies of mRNA splicing at the various 5ôSSs of intron 11 were estimated by RTï PCR analysis, using the primers represented in panel A. The amplified products were fractionated by gel-electrophoresis. The identities of the constructs used are given above the lanes. Overexpression of SRSF1 or SRSF5 in HeLa cells is indicated by +. Lengths in bps of size markers are indicated. Positions of products resulting from utilization of the LMNA, progerin or LAΔ35 5ôSSs are shown on the right side of the gel. **(C)** Quantification of the rate of laminA, progerin and LAΔ35 5ôSS utilization in 4 independent experiments including the one exemplified in Panel B. The yields of utilization of the different splice sites in a given assay are expressed as the percentage of amplified product corresponding to utilization of this splice site versus the total amount of amplified products. The percentages given in this panel correspond to the mean values of four independent transfection assays. Standard deviations are given. **(D)** Quantification of the percentage of utilization of the progerin and LMNA 5ôSSs in dose effect experiments performed with the

1824C>T (left panel), 1822G>A (middle panel) and 1868C>G *βglo* LMNA constructs (right panel). HeLa cells were co-transfected with one of *βglo* LMNA constructs and increasing amounts of the pXJ41-SRSF5 or increasing amounts of pXJ42-SRSF7 plasmid as a control.

Figure 3: In *in vitro* splicing assays, SRSF5 activates LMNA 5ʹSS utilization in the presence of all three HGPS mutations

(A and B) Splicing assays were performed using the WT, 1822G>A 1868C>G (Panels A and B) and 1824C>T (Panel B) *βglo*-LMNA reporter transcripts and HeLa nuclear extracts without (Panel A, lanes 1, 5 and 8 and Panel B, lanes 1, 4, 7 and 10) or with addition of recombinant SRSF1 (Panel A, 200 ng in lanes 2, 6 and 9 or 400 ng in lanes 3, 7 and 10) or SRSF5 (Panel B, 200 ng in lanes 2, 5, 8 and 11 or 400 ng in lanes 3, 6, 9 and 12). Splicing products were separated on polyacrylamide denaturing gels. The identity of the splicing product is indicated on the left side of the autoradiograms. Lengths in bps of size markers are indicated. Quantification of the rate of utilization of the laminA, progerin and LAΔ35 5ʹSS in these experiments are given on the right side of each Panel. Relative amounts are expressed as percentage of the total amount of spliced RNAs.

Figure 4: Enhanced expression of SRSF5 in dermal fibroblasts of a HGPS patient reduces progerin 5ʹSS utilization.

(A) Western blot analysis using the anti-SR (1H4) specific antibody showing the overexpression of SRSF5 in dermal fibroblasts of a HGPS patient. Proteins SRSF6 and SRSF1 were used as loading controls. **(B)** Quantification of the effect of SRSF5 overexpression in HGPS fibroblasts on the relative ratios of the endogenous progerin and lamin A mRNAs. Cells were electroporated with plasmid pXJ41 (control assay) or pXJ41-SRSF5 (assay). Total RNAs were extracted 24 hours later. Levels of lamin A and progerin mRNAs were estimated by RT-

PCR using two primers located in exons 8 and 12, respectively. The mean values of 6 independent experiments are given. The standard deviation is indicated. The statistical significance was determined using a studentôs t-test (pÒ0.01 = **).

Figure 5: PDGF-BB treatment reduces LMNA splicing defects and nuclei morphological abnormalities in HGPS fibroblasts.

(**A-B-C-D-E)** Effect of four days stimulation with PDGF-BB (40 ng/ml) on intron 11 5ôSS utilization, progerin/ Lamin A mRNA and protein ratio and nuclear shape in dermal fibroblasts of a HGPS patient. **(A)** Relative yields of utilization of progerin *versus* LMNA 5ôSS utilization in dermal fibroblasts from an HGPS patient. Total RNAs were isolated and the levels of lamin A and progerin mRNAs were determined by gel electrophoresis of RT-PCR amplified fragments obtained with the same primers as in Figure 4. A size marker was fractionated in parallel (Lane M, length in pbs). The progerin/Lamin A mRNA ratios given in this panel are represented as the fold change observed upon PDGF-BB treatment (n=4; pÒ0.01 = **). **(B)** Western blot analysis of the effect of PDGF-BB treatment on the relative amounts of Lamin A and progerin in HGPS fibroblats. A mouse anti-lamin A/C antibody (Santa Cruz Biotechnologiy, sc-20681) was used to detect both lamin A, progerin and lamin C. The progerin/Lamin A protein ratios given in this panel are represented as the fold change observed upon PDGF-BB treatment (n=3; pÒ0.05 = *). GAPDH was used as a loading control. **(C-D-E)** PDGF-BB treatment decreased morphological abnormalities of HGPS cell nuclei. **(C)** Representative immunofluorescence images of the nuclei of HGPS cells at passage 16 and of control fibroblasts both treated with PDGF-BB or with vehicle (mock) are shown. Cell nuclei were labelled using mouse anti-lamin A/C antibody (Santa Cruz Biotechnology, Inc. #sc-20681). Imaging was performed using a Nikon Optiphot-2 fluorescence microscope. **(D)** PDGF-BB treatment reduced the frequency of cells presenting with abnormal nuclear shape.

The percentage of cells with aberrant nuclear shape was scored by two blinder observers who counted four independent data sets of 150 to 270 lamin A/C labelled nuclei for each condition. The mean values of the 4 independent experiments are given. **(E)** Automated analysis of the effects of PDGF-BB treatment on nuclear morphology using two Image J complementary shape descriptors. The solidity and aspect ratio of cell nuclei were compared for mock-treated control fibroblasts *versus* HGPS cells and for HGPS cells without (-) PDGP-BB treatment *versus* HGPS cells with (+) PDGF-BB treatment. Solidity (area/convex area; no invagination = 1) decreases as nuclei become more lobulated. The aspect ratio (major axis/minor axis; circle = 1) increases with the elongation of the fitted ellipse. Representative data from one data set corresponding to 260 cells are shown. The statistical significance was determined using a studentôs t-test (pÒ 0.001 = ***). The standard deviation is indicated.

A

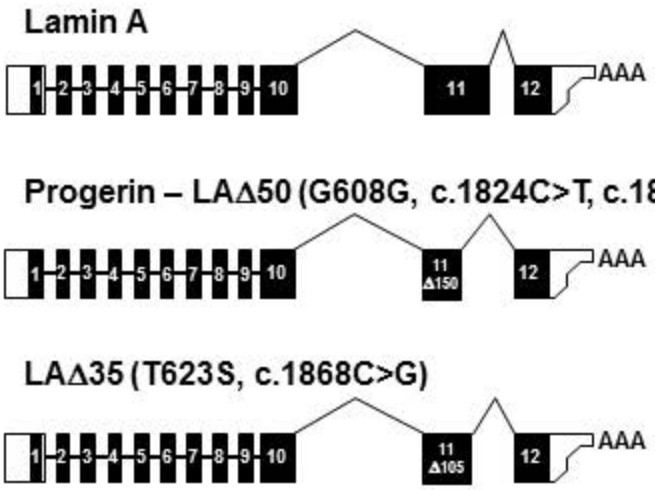

B

	MaxEnt score	Analyzer Splice Tool	SS score calculation	5'ss sequence
Consensus 5'SS	10.86	100,00	12,4	CAG/GTAAGT
Lamin A 5'SS	10.67	95,04	12,2	CAG/GT**G**AGT
Progerin 5'SS	8.07	79,04	7,1	CAG/GT**GG**GC
Progerin 5'SS+ 1824C>T	8.56	84,90	9,2	CAG/GT**GG**GT
Progerin 5'SS + 1822G>A	9.60	89,18	10,1	CAG/GT**G**AGC
LAΔ35 5'SS	0.44	67,92	0,1	**A**CG/GTCACT
LAΔ35 5'SS + 1868C>G	8.02	78,40	3,8	**A**CG/GTCAGT

Figure 1. Vautrot *et al*

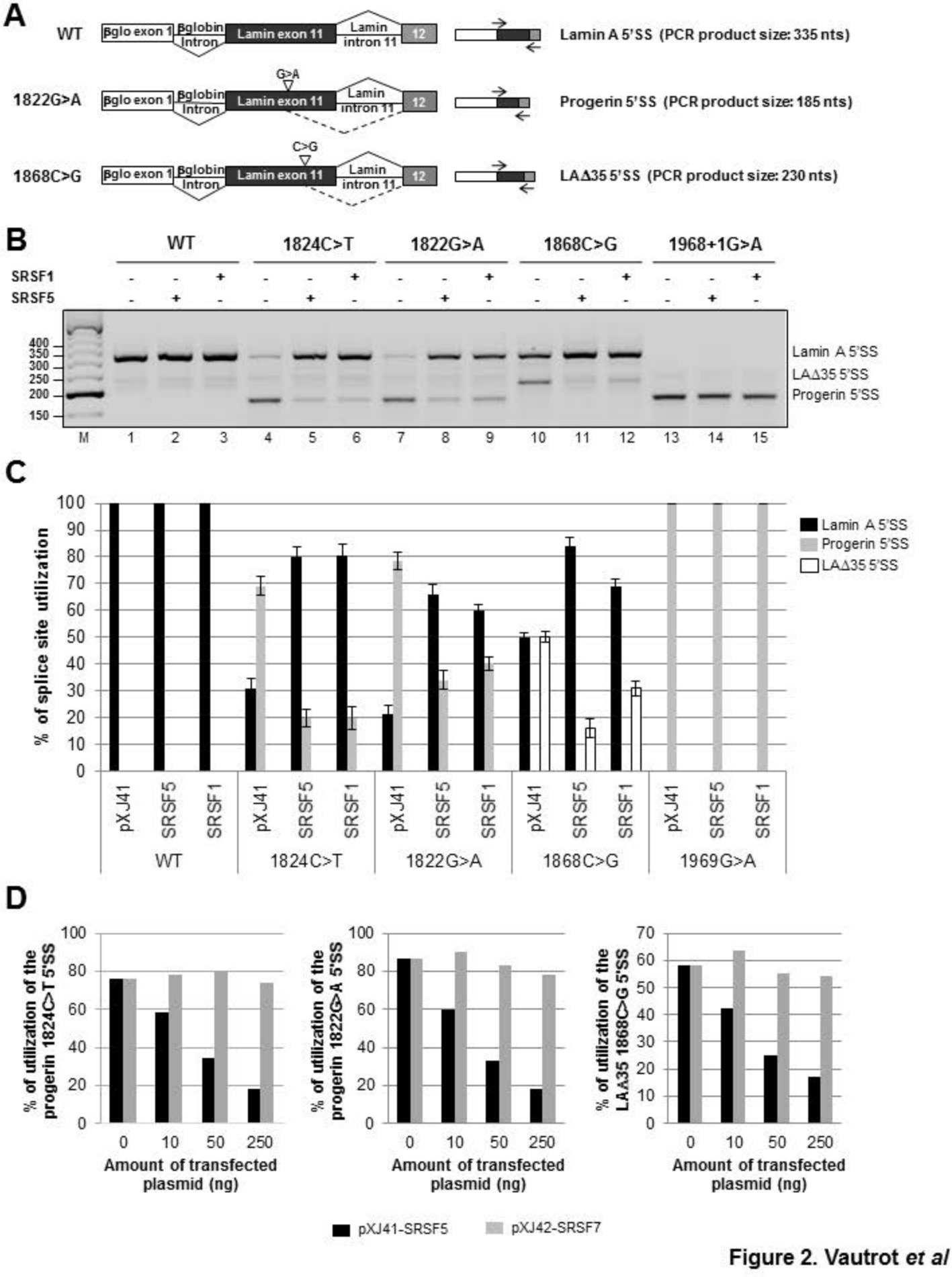

Figure 2. Vautrot *et al*

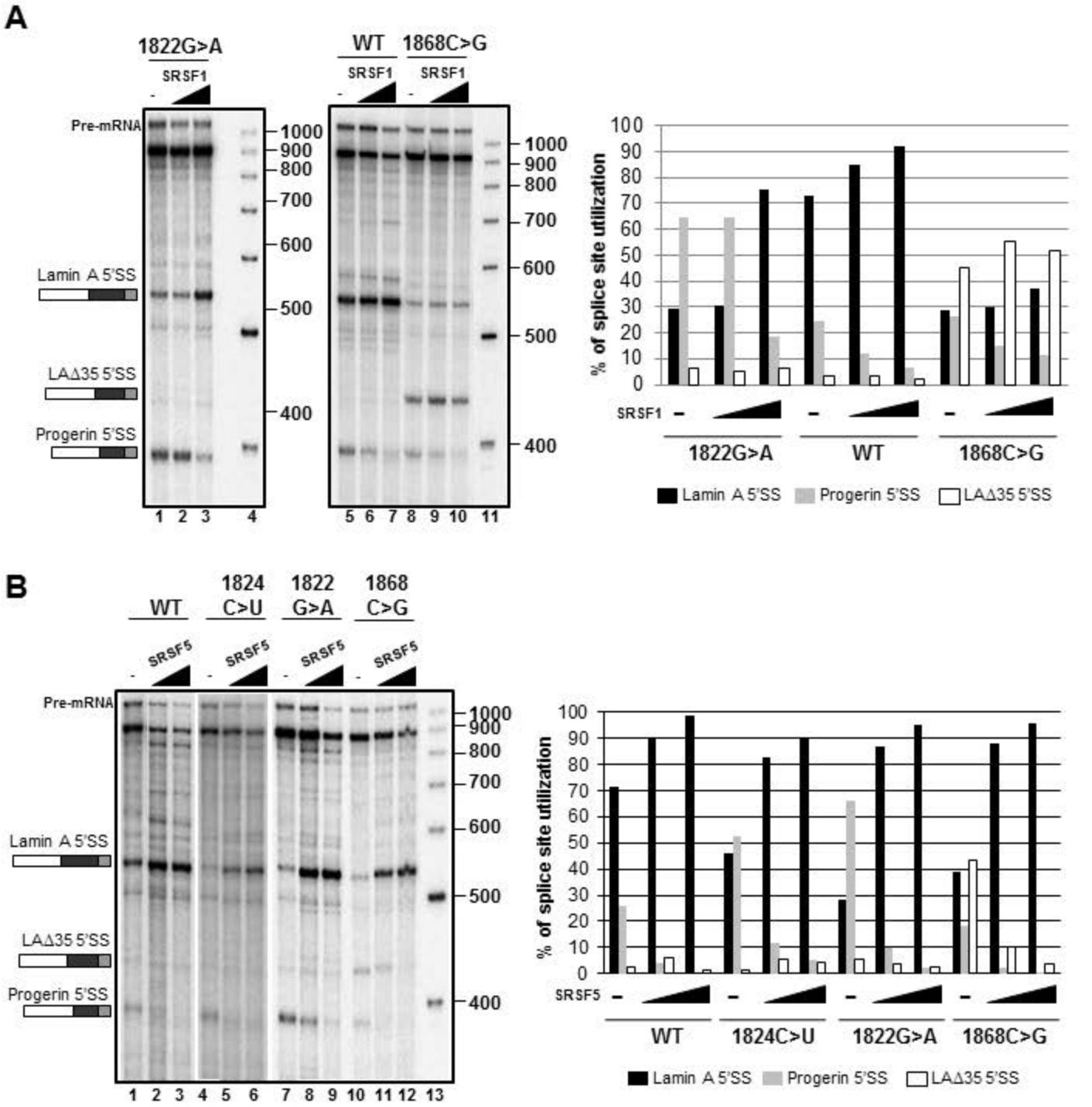

Figure 3. Vautrot *et al*

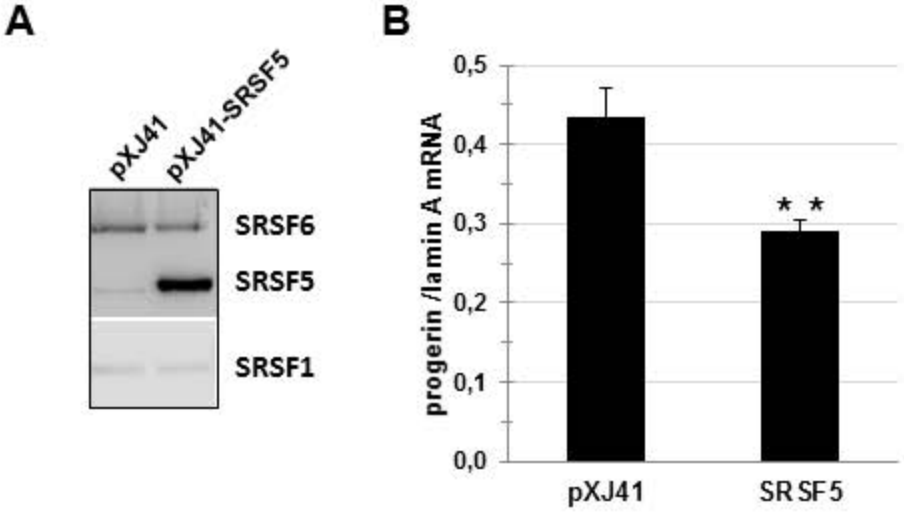

Figure 4. Vautrot *et al*

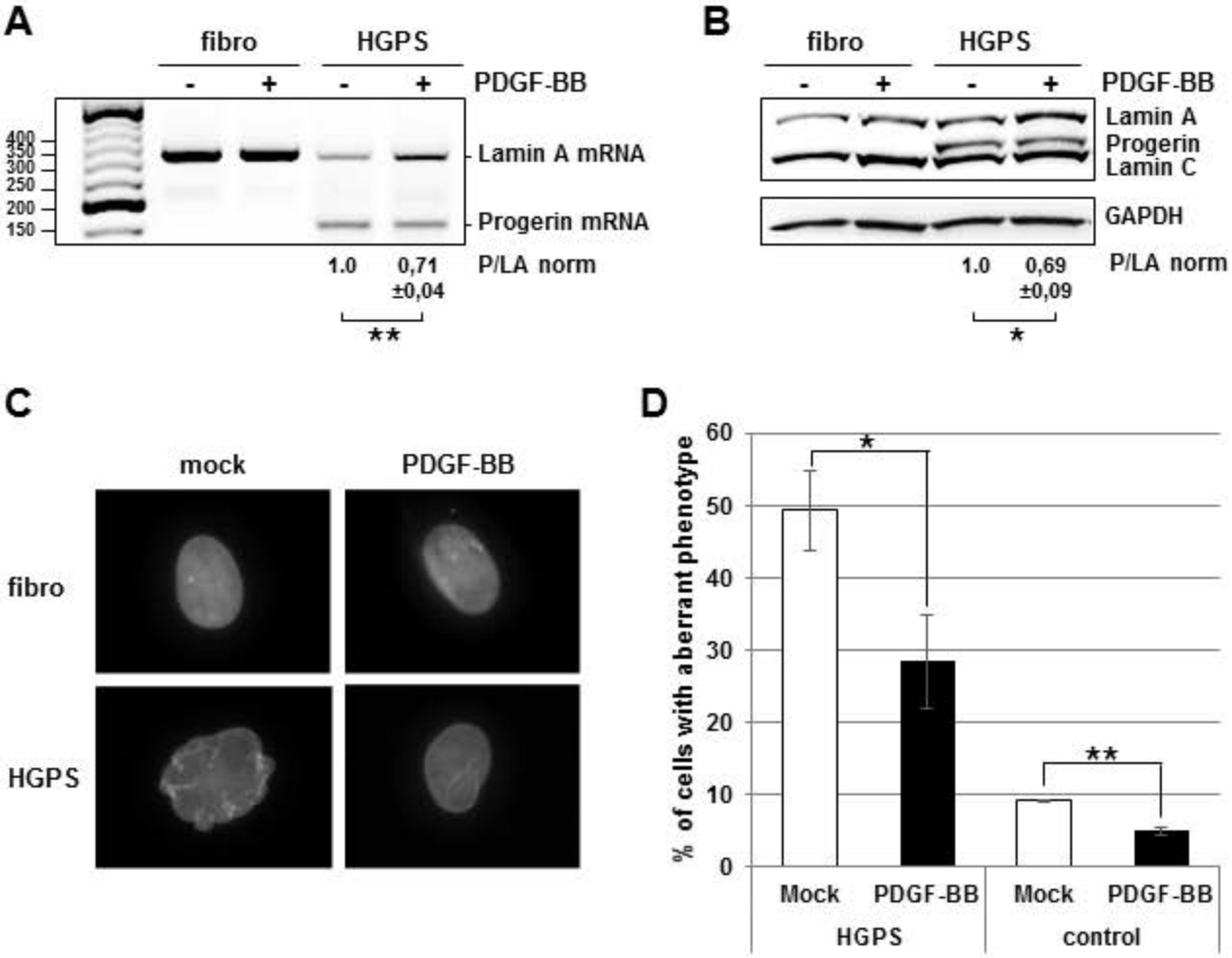

E

	Solidity		Aspect ratio	
cells	Mean value ± SEM	p-value	Mean value ± SEM	p-value
Control vs HGPS	0.9916 ± 0.0002 vs 0.9817 ± 0.0011	1.76E-15	1.49 ± 0.01 vs 1.30 ± 0.01	1.52E-19
HGPS -/+ PDGF-BB	0.9817 ± 0.0011 vs 0.9861 ± 0.0005	8.13E-04	1.30 ± 0.01 vs 1.40 ± 0.01	2.06E-07

Figure 5. Vautrot *et al*

Supporting Methods

In silico prediction methods

Three different freely available bioinformatics tools have been used to evaluate the strength of the 5ô splice sites present within exon and intron 11 of the *LMNA* gene. The MaxEntScan::score5SS (MES; http://genes.mit.edu.gate1.inist.fr/burgelab/maxent/Xmaxentscan_scoreseq.html) algorithm is based on maximum entropy distribution [Yeo and Burge, 2004]. It scores 9-mer sequences corresponding to positions {-3 to +6} of the 5ôSS (i.e. last 3 bases of the exon and the first 6 bases of succeeding intron), which have the GT consensus at positions {+1,+2}. Using this algorithm, the perfect 5ôSSs AAG/gtaagt and CAG/gattgt will have scores of 11.0 and 10.86, respectively and the scores range from 0 to 11.0 [Yeo and Burge, 2004]. The Analyzer Splice Tool (http://ibis.tau.ac.il/ssat/SpliceSiteFrame.html) scores also 9-mers but using a position weight matrix score calculated by comparison to a data set of 45519 homologous human-mouse U2-dependent 5ôSS sequences with GT at the invariant positions of introns for which their upstream exon is constitutively spliced and for which they share the same reading frame [Shapiro and Senapathy, 1987; Carmel et al., 2004]. The score expresses how similar the splice-sites fit the consensus sequences and thus the perfect 5ôSS CAG/gattgt will give a score of 100. The Splice Site Score Calculation (http://rulai.cshl.edu/new_alt_exon_db2/HTML/score.html) also scores 9-mers. The given score expresses how similar the splice site fits the consensus sequence. A 100 % match to the mammalian perfect 5ôSS AAG/gtaagt will have a score of 12.6 and the mean score of the 5ôsplice site in constitutive exons is 8.1.

Morphometric analysis of cell nuclei

A custom-written Image J (National Institutes of Health, Bethesda, MD) algorithm based on the MATLAB script described by Driscoll et al. was used to extract nuclei boundaries of lamin

A/C labelled cells and to measure nuclei shape descriptors [Driscoll et al., 2012]. To reduce image histogram variability both between and within images, a contrast-limited adaptive histogram equalization was applied by using the «Auto Image J » function that automatically optimizes brightness and contrast. Next, images were binarized using the Image Jôs built-in thresholding function, which uses Minimumôs method. Holes within bright regions were then filled, and regions that either overlapped the image boundary or were smaller than 15000 square pixels were removed. Fitting a cubic spline curve with sub-pixel resolution to these polygon selections from binary images made these regions smoothed perfectly with the nuclei boundaries. Nuclei morphometric parameters, including area, perimeter, solidity and aspect ratio were then measured using Image J. Solidity (area/convex area) provides a sense of the nuclei irregularity. It is equal to 1 for nuclei with no invagination (convex) and decreases as nuclei become more lobulated. The solidity of multilobed HGPS fibroblast nuclei is thus expected to be smaller than the one of control fibroblasts [Choi et al., 2011; Booth-Gauthier et al., 2013]. Aspect ratio (major axis/minor axis) is a measure of the cell elongation. The aspect ratio for a circle is equal to 1 and increases with the elongation of the fitted ellipse. The fact that control fibroblast nuclei are generally more ovoid than HGPS nuclei results in an aspect ratio value higher than for HGPS cells [Barthelemy et al., 2015; Choi, et al., 2011; Booth-Gauthier, et al., 2013].

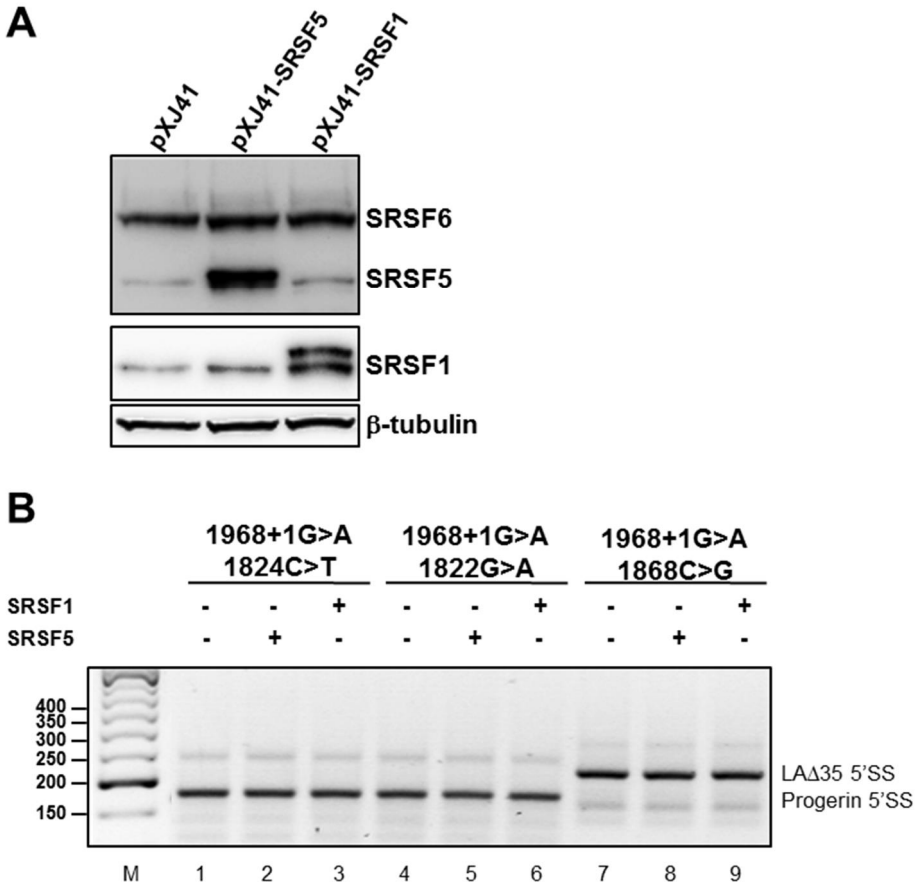

Supp. Figure S1: Validation of the over-expression of the SRSF1 and SRSF5 proteins in HeLa cells and analysis of its effects on intron 11 5ô SS utilization in mutated *βglo* LMNA transcripts.

(A) Western blot analysis of SRSF1 and SRSF5 expression upon co-transfection of HeLa cells with plasmids pXJ41-SRSF1 and pXJ41-SRSF5, respectively. The β-tubulin was used as a control. Cells were collected 24 hours after transfection, proteins were extracted and fractionated by SDS-PAGE and revealed using the anti-SR (1H4) (top panel) and the anti-SRSF1 (bottom panel) antibodies. The two bands detected after SRSF1 overexpression correspond mainly to the His-tagged SRSF1 **(B)** Co-transfection of HeLa cells with empty pXJ41, pXJ41-SRSF1 or pXJ41-SRSF5 plasmid and one of the minigene reporters *βglo*-LMNA carrying the 1968+1G>A mutation in combination with either the 1824C>T, 1822G>A or 1868C>G mutation. The splicing products were investigated by RTï PCR analysis of RNA extracted from transfected cells using the same primers as in Figure 2.

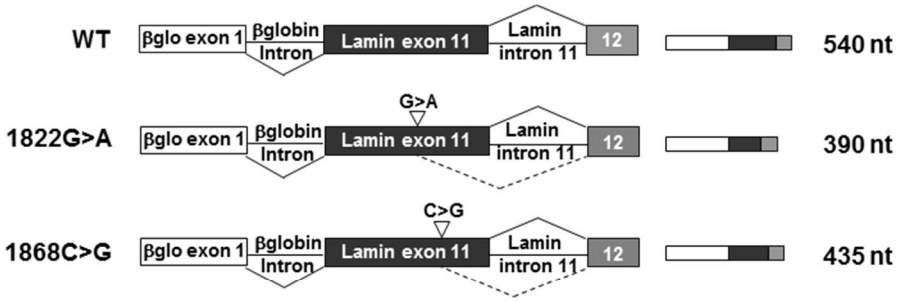
WT
βglo exon 1
βglobin Intron
Lamin exon 11
Lamin intron 11
12
540 nt
1822G>A
G>A
390 nt
1868C>G
C>G
435 nt

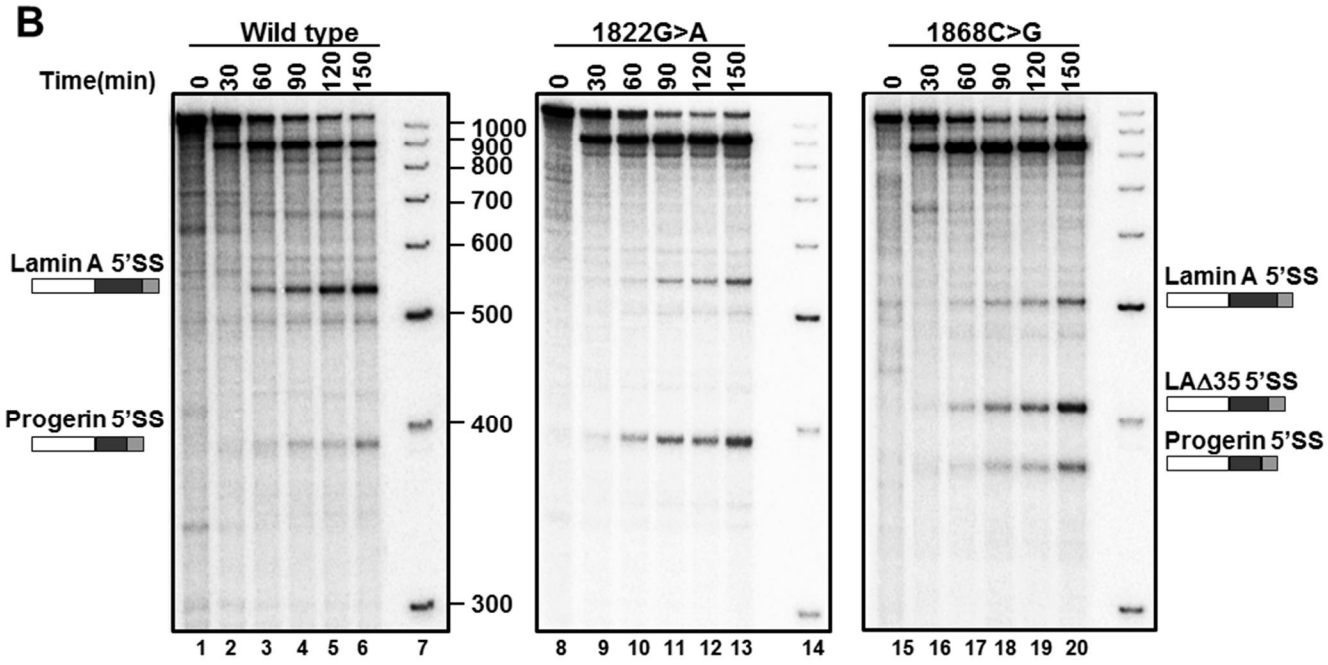
B
Wild type
1822G>A
1868C>G
Time(min)
0 30 60 90 120 150
Lamin A 5'SS
Progerin 5'SS
LAΔ35 5'SS
1000
900
800
700
600
500
400
300
1 2 3 4 5 6 7
8 9 10 11 12 13 14
15 16 17 18 19 20

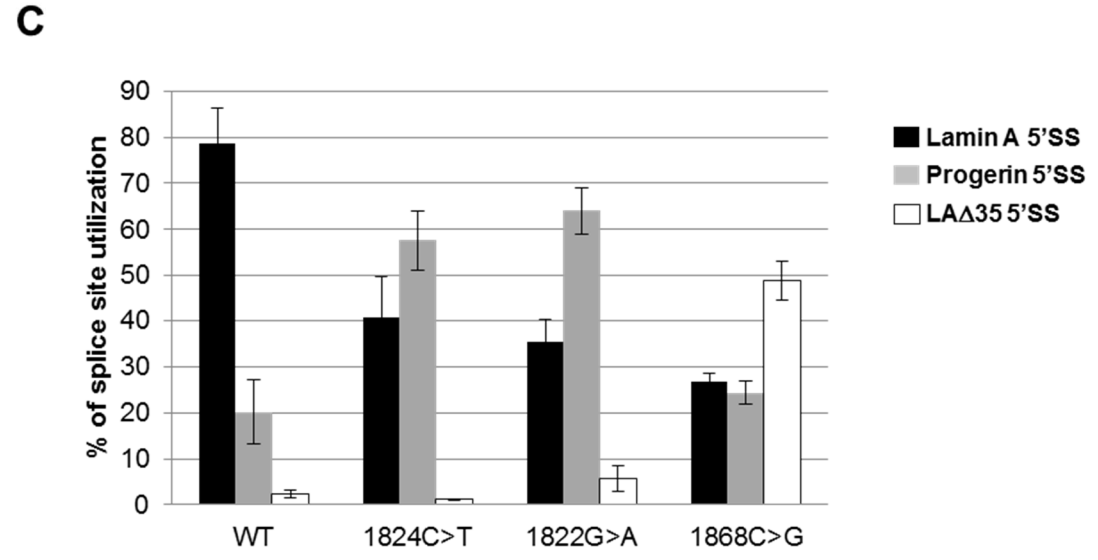
C
% of splice site utilization
90
80
70
60
50
40
30
20
10
0
WT
1824C>T
1822G>A
1868C>G
Lamin A 5'SS
Progerin 5'SS
LAΔ35 5'SS

Supp. Figure S2: Time course analyses of *in vitro* splicing of WT, 1822G>A and 1868C>G βglo-LMNA transcripts.

(A) Schematic representation of the *βglo*-LMNA substrates used for *in vitro* splicing assays. The sizes of the expected splicing products are indicated. **(B)** Time course analysis of *in vitro* splicing in Hela cellôs nuclear extracts of WT, 1822G>A and 1868C>G radiolabeled *βglo*-LMNA reporters showing the kinetics of lamin A, progerin and LAΔ35 5ôSS utilizations in the various genetic contexts. The identity of mature RNAs are indicated on the right sides of the autoradiograms. The same mixture of size markers was loaded on each gel (left lane) and their sizes in pbs are indicated. Durations of the incubations in minutes are indicated on top of each autoradiograms. **(C)** Quantification, of the relative amounts of the laminA, progerin and LAΔ35 5ôSS RNAs produced after 120 min of splicing reaction. Relative amounts are expressed as percentage of the total amount of spliced RNA.

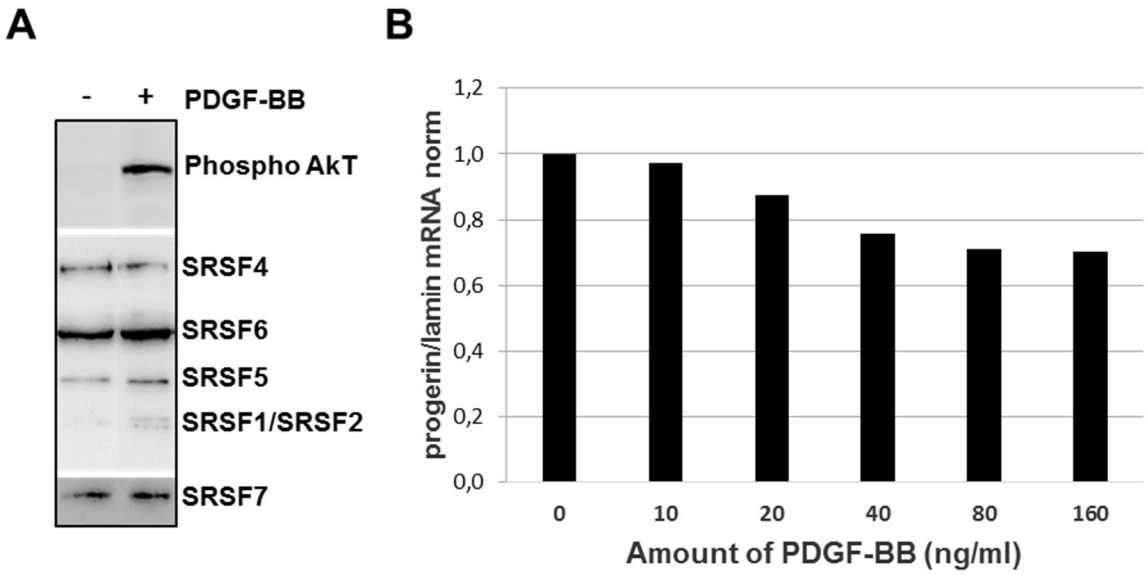

Supp. Figure S3: PDGF-BB treatment changes the phosphorylation status of Akt and some SR proteins and modulates LMNA splicing in a dose-dependent manner.

(A) Western blot analysis using anti-PhosphoAkt, anti-SR (1H4) and anti-SRSF7 antibodies of the effect of 24 hours stimulation with PDGF-BB (20 ng/ml) on the phosphorylation status of Akt and of various SR proteins identified according to their electrophoretic mobilities. **(B)** PDGF-BB dose effect on the utilization of the progerin and LMNA 5ôSSs. Relative yields of utilization of progerin *versus* LMNA 5ôSSs in dermal fibroblasts from an HSPG patient stimulated for 24 hours with increasing amount of PDGF-BB. The ratios of progerin/Lamin A mRNAs given in this panel are represented as the fold change relative to HGPS cells without PDGF-BB treatment

Supp. references

Barthelemy F, Navarro C, Fayek R, Da Silva N, Roll P, Sigaudy S, Oshima J, Bonne G, Papadopoulou-Legbelou K, Evangeliou AE, Spilioti M, Lemerrer M, et al. 2015. Truncated prelamin A expression in HGPS-like patients: a transcriptional study. Eur J Hum Genet.

Booth-Gauthier EA, Du V, Ghibaudo M, Rape AD, Dahl KN, Ladoux B 2013. Hutchinson-Gilford progeria syndrome alters nuclear shape and reduces cell motility in three dimensional model substrates. Integr Biol (Camb) 5: 569-577.

Carmel I, Tal S, Vig I, Ast G 2004. Comparative analysis detects dependencies among the 5' splice-site positions. RNA 10: 828-840.

Choi S, Wang W, Ribeiro AJ, Kalinowski A, Gregg SQ, Opresko PL, Niedernhofer LJ, Rohde GK, Dahl KN 2011. Computational image analysis of nuclear morphology associated with various nuclear-specific aging disorders. Nucleus 2: 570-579.

Driscoll MK, Albanese JL, Xiong ZM, Mailman M, Losert W, Cao K 2012. Automated image analysis of nuclear shape: what can we learn from a prematurely aged cell? Aging (Albany NY) 4: 119-132.

Shapiro MB, Senapathy P 1987. RNA splice junctions of different classes of eukaryotes: sequence statistics and functional implications in gene expression. Nucleic Acids Res 15: 7155-7174.

Yeo G, Burge CB 2004. Maximum entropy modeling of short sequence motifs with applications to RNA splicing signals. J Comput Biol 11: 377-394.